HOKKAIDO UNIVERSITY

Title	Liquid-phase syntheses of sulfide electrolytes for all-solid-state lithium battery
Author(s)	Miura, Akira; Rosero-Navarro, Nataly Carolina; Sakuda, Atsushi et al.
Citation	Nature Reviews Chemistry, 3(3), 189-198 https://doi.org/10.1038/s41570-019-0078-2
Issue Date	2019-02-19
Doc URL	https://hdl.handle.net/2115/76128
Type	journal article
File Information	Accept Manuscript. DOI 10.1038s41570-019-0078-2.pdf

Hokkaido University Collection of Scholarly and Academic Papers : HUSCAP

Accepted Manuscript: *Nature Reviews Chemistry,* **3**, pages189–198 (2019) 10.1038/ s41570-019-0078-2

Liquid-phase syntheses of sulfide electrolytes for all-solid-state lithium battery

Akira Miura[a)], Nataly Carolina Rosero-Navarro[a)], Atsushi Sakuda[b)], Kiyoharu Tadanaga[a)*], Nguyen H.H. Phuc[c)], Atsunori Matsuda[c)], Nobuya Machida[d)], Akitoshi Hayashi[b)], Masahiro Tatsumisago[b)*]

a)Faculty of Engineering, Hokkaido University, Kita 13 Nishi 8, Sapporo 060-8628, Japan, b) Department of Applied Chemistry, Graduate School of Engineering, Osaka Prefecture University, 1-1 Gakuen-cho, Sakai 599-8531, Japan. c) Department of Electrical and Electronic Information Engineering, Toyohashi University of Technology, 1-1 Hibarigaoka, Toyohashi 441-8580, Japan. d) Department of Chemistry, Konan University, Okamoto 8-9-1, Kobe 658-8501, Japan,

ABSTRACT: Solid sulfide electrolytes are key materials in all-solid-state lithium batteries because of their high Li ion conductivity and deformability that enables Li ion path to be connected between the grains by pressing the materials near room temperature. However, sulfur species are moisture-sensitive and exhibit high vapor pressures, therefore syntheses of sulfide electrolytes need to be carefully designed. Liquid-phase reactions can be performed at low temperatures in controlled atmospheres, opening up the prospect of scalable processes for the preparation of sulfide electrolytes. Here, we review liquid-phase syntheses for the preparation of sulfide-based solid electrolytes and composites of electrolytes and electrodes, and we compare charge-discharge performances of the all-solid-state lithium batteries using these components.

1. Introduction

High-energy density and long cycle life in rechargeable batteries are highly demanded, especially for electronic vehicles and for large-scale power storage to balance the electrical grid using renewable energy. Lithium batteries can achieve high energy density per weight because lithium is the lightest solid element at room temperature under ambient pressure and is characterized by low reduction potential. However, the flammable organic electrolytes in lithium ion batteries pose safety issues and limit the batteries' temperature range of operation. Last decades have seen the development of all-solid-state lithium batteries that can solve these safety concerns by avoiding the use of flammable electrolytes.[1-5] The use of solid electrodes can help achieve high lithium conductivity as only lithium ions are transported in the solid-frameworks without the diffusion of anions. A breakthrough in this area was the discovery of solid electrolytes with high lithium-ion conductivities, which include:[4, 6-9] glasses and glass ceramics,[10-12] $Li_{14}Zn(GeO_4)_4$/$Li_{4-x}Ge_{1-x}P_xS_4$ and their analogs (so-called LISICON/thio-LISICON),[11-15] Li_6PS_5Cl and isostructural compounds (argyrodites),[16-17] $La_{2/3-x}Li_xTiO_3$ and related perovskites[18], $Li_{1+x}Al_xTi_{2-x}(PO_4)_3$-related compounds (so-called NASICON)[19], and $Li_7La_3Zr_2O_{12}$ and isostructural compounds (garnets).[20-21] Solid electrolytes are stable over a wide temperature range and can be coupled with electrodes in the range of wide voltage. The all-solid-state cell composed of sulfide electrodes and sulfide electrolyte operates as a secondary battery over a wide temperature range -30–160 °C.[22]; no significant degradation due to dissolution of sulfide electrode into solid electrolyte occur even at high temperature.

Sulfide-based solid electrolytes show excellent lithium conductivities, in some cases even higher than those of liquid organic electrolytes.[15] Moreover, sulfide electrolytes are more deformable than oxide electrolytes[23]. The grain boundary resistance of sulfide electrolytes can be decreased just by pressing the material at room temperature or at moderate temperature below 200 °C.[24-25] Furthermore, sulfide electrolytes can form low-resistive interfaces between electrodes coated with an effective buffer layer and electrolytes in composite electrodes consisting of electrodes and electrolytes.[26]

Most sulfide-based electrolytes are not stable in water leading to the evolution of H_2S gas (although this instability can be improved by modifying or changing the electrolyte compositions[27-29]) and making the synthetic processes complex..[30] Usually, starting materials and products are handled in an Ar-filled glovebox.[15-16] In lab-scale syntheses, evacuated quartz ampoules are commonly used for heat treatment to prevent the release of sulfur species with relatively high vapor pressure. However, the use of quartz ampoules makes the scale up of such synthetic approaches difficult. High-energy ball-milling syntheses near room temperatures have also been developed.[10] These do not involve high-temperature treatments. Nonetheless, the amount of product is limited by the size of the ball-milling jar and synthesis are typically performed over 8–50 hours.[10, 17]

Liquid-phase syntheses have been proposed for the production of metal sulfides and chalcogenides (such as ZnS, CdSe) and their clusters to be used in electronic devices, solar cells, and biological probes.[31-33] There has been limited work until 2012 on liquid-phase chemistry with thiophosphates, which are the main components of Li-conducting sulfide electrolytes .[34-35] More recently, more attention has been payed to liquid-phase syntheses and these have been used for the preparation of solid electrolytes. Liquid-phase syntheses present several advantages with respect to solid-sate ones in terms of synthesis temperature, synthesis time, and scalability. Liquid-phase syntheses are usually performed below 300 °C, a much lower temperature than that required by solid-state synthesis, which is typically above 500 °C.[15-16] Liquid-phase syntheses can be performed in a glass container, with the vapor pressure of sulfur species being low. Moreover, they can lead to the formation of metastable phases with high lithium conductivities, such as $Li_7P_3S_{11}$.

Liquid-phase processes are also attractive for producing composites of electrolytes and electrodes in all-solid-state lithium batteries. The composite positive electrodes prepared by milling using a mortar and pestle need to be typically mixed with 30–60 wt% solid electrolyte to maintain lithium conduction pathways to the electrodes.[36-37]Indeed, the minimum amounts of solid electrolytes that sustain lithium conduction pathways should be used to maximize the energy densities of all-solid-state batteries. Initial studies of model active material particles coated with a thin electrolyte were conducted using pulse laser deposition (PLD).[38-40] However, PLD is performed under a high vacuum conditions, limiting the scaling up of the process. Liquid-phase processes have potentials for scalability because solutions cover the surfaces of electrodes, electrode composites are formed during the subsequent heating processes. Furthermore, mixing of electrodes, electrolyte, and electron conductors does not require the use of special apparatuses and low-temperature treatments prevent undesirable reactions between electrodes and sulfide electrolytes.

In this Review, we report on the progress of liquid-phase synthesis of sulfide electrolytes for all-solid-state lithium battery . We categorize these into two groups(FIG. 1):[5] first, we focus on suspension synthesis of sulfide electrolytes from Li_2S and P_2S_5 in organic solvents. Second, we introduce the dissolution–precipitation of sulfide electrolytes using solvents in which they are highly soluble. Finally, we summarize the liquid-phase processes and the performances of all-solid-state lithium batteries using composite electrodes produced by liquid-phase routes.

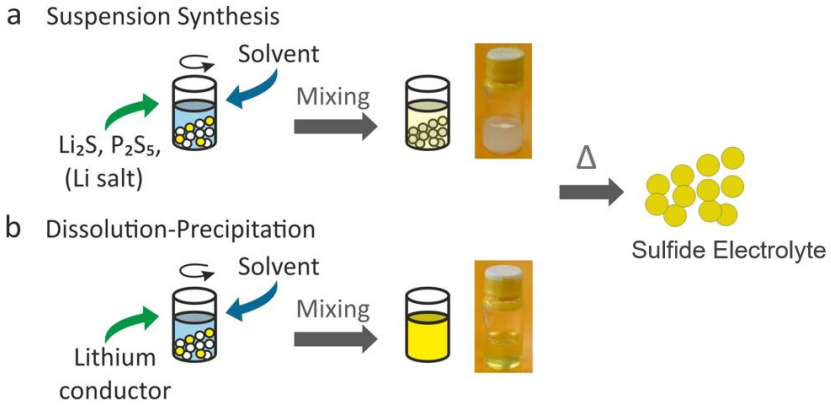

Figure.1 Schematic of liquid-phase syntheses of sulfide electrolytes. **a**| In the suspension syntheses, precursors such as Li_2S and P_2S_5 are suspended through mixing in organic solvents, such as 1,2-dimethoxyethane (DME), tetrahydrofuran (THF), acetonitrile (ACN), ethyl acetate (EA), dimethyl carbonate (DMC), and ethyl propionate (EP), in which the precursors are not highly soluble. Li_2S and P_2S_5 form complexes in solution, which are allowed to precipitate through heating and consequent evaporation of the solvent **b**| In the dissolution–precipitation approach the solid electrolyte is complexly dissolved in solvents such as hydrazine, N-methylformamide (NMF), methanol, and ethanol. Heating enables the precipitation of the solid sulfinde electrolytes.

2. Liquid-phase reactions for solid electrolytes

2-1. Suspension syntheses

Most of the syntheses of solid electrolytes using the suspension approach (table 1) have been performed to produce Li_2S–P_2S_5 solid electrolytes, for which Li_2S and P_2S_5 are the precursors. The precursors are dispersed in organic solvents such as: 1,2-dimethoxyethane (DME), tetrahydrofuran (THF), acetonitrile (ACN), ethyl acetate (EA), dimethyl carbonate (DMC) and ethyl propionate (EP). Dispersed Li_2S and P_2S_5 form complexes (Fig. 2a), although partial dissolution of precursors, intermediates and their complexes might occur (Fig. 2b) as shown in few studies that reported a complete dissolution of the intermediates and the precipitation of the products.[41-43] Solid–liquid separation or solvent evaporation result in the formation of solid complexes such as Li_3PS_4·3THF and further heating at 60–300 °C removed organic solvents to form sulfide electrolytes. Because Li_2S and the synthesized sulfide electrolytes are highly water sensitive, they are handled in an inert atmosphere, typically in an Ar-filled glovebox.

In 2013, Liang and co-workers reported the synthesis of nanoporous β-Li_3PS_4 (FIG. 2**c**) using THF as solvent.[44] Overnight stirring of Li_2S and P_2S_5 in THF and subsequent centrifugation produced Li_3PS_4·3THF complex. Further heating at 80 °C decomposed this complex, resulting in the formation of amorphous Li_3PS_4 with ionic conductivity of 7.4×10^{-5} S cm^{-1}. After heating at 140 °C, nanoporous β-Li_3PS_4 was formed. Three polymorphs of Li_3PS_4 can be attained through solid-state reaction: α, β, and γ-Li_3PS_4 phases that corresponds to high to low-temperature modifications, with β-Li_3PS_4 phase being only observed in the narrow temperature range 300–485 °C.[45] This means that suspension synthesis leads to a thermodynamically metastable phase at low temperature. Lithium ion conductivity of β-Li_3PS_4 is 1.6×10^{-4}

S cm^{-1} at 25 °C, which is higher than that of thermodynamically stable γ-Li_3PS_4 (3.0 × 10^{-7} S cm^{-1})[45]. Facetted particles of Li_3PS_4·3THF complex were a few tens of microns in size, which were similar to β-Li_3PS_4 particles (FIG. 2**c**). Nonetheless, nano-sized pores were observed on the surface of β-Li_3PS_4 particles, resulting in high surface area. In 2014, the same group also reported the liquid-phase synthesis of a new phase, $Li_7P_2S_8I$, using ACN.[46] The synthesis involved the formation of Li_3PS_4·2ACN complex in ACN solvent over 24 hours, mixing of this complex with LiI in ACN and subsequent heating at 200 °C. $Li_7P_2S_8I$ exhibited a ionic conductivity of 6.3 × 10^{-4} S cm^{-1} and high stability toward metallic lithium.

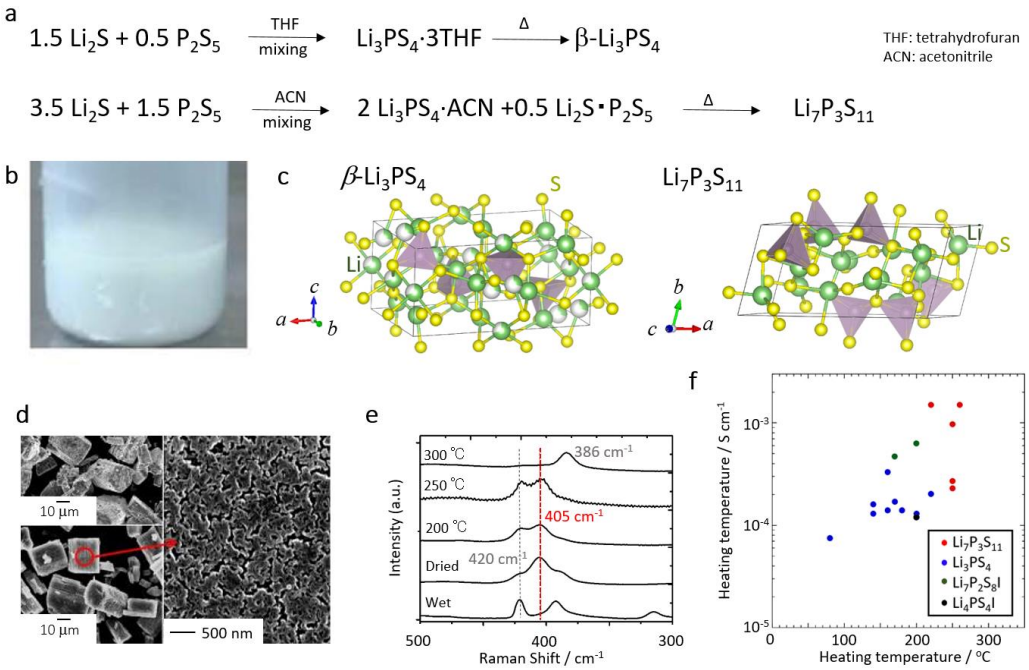

Figure 2 Suspension synthesis of sulfide electrolyte. **a** Suspension reactions for the synthesis of representative solid sulfide electrolytes.[43-44] **b** Photo of suspension for the $Li_7P_3S_{11}$ precursors. **c** On the left, crystal structure of β-Li_3PS_4 with tetrahedrons being PS_4^{3-}.[45, 79] On the right, crystal structure of $Li_7P_3S_{11}$ with PS_4^{3-} and $P_2S_7^{4-}$ units. [79-80]**d** Faceted Li_3PS_4·3THF particles (top)[44], β-Li_3PS_4 particles, which have a morphology similar to that of Li_3PS_4·3THF particles (bottom)[44] and β-Li_3PS_4 surface featuring nanopores.[44] **e** Raman spectra of the various steps of the suspension synthesis of Li_2S–P_2S_5 powder synthesized.[47] Peaks at 420, 405 and 386 cm^{-1} are attributed to PS_4^{3-}, $P_2S_7^{4-}$ and $P_2S_6^{4-}$, respectively. PS_4^{3-} and $P_2S_7^{4-}$ in $Li_7P_3S_{11}$ phase are detected after drying and subsequent heating at 200 and 250°C. **f** Heating temperatures for suspension synthesis and the corresponding conductivities of synthesized electrolytes near room temperature.[41-42, 44, 46-52, 54-56, 59, 81]

TABLE 1 Suspension synthesis of sulfide-based solid electrolytes and their conductivities near room temperature.

Product	Reactant	Solvent	Temp. (°C)	σ (mS cm^{-1})	Ref.
a-Li_3PS_4*	Li_2S, P_2S_5	THF	80	0.074	44
β-Li_3PS_4	Li_2S, P_2S_5	THF	140	0.16	44
β-Li_3PS_4	Li_2S, P_2S_5	EA	160	0.33	50
β-Li_3PS_4	Li_2S, P_2S_5	ACN	200	0.12	51
β-Li_3PS_4	Li_2S, P_2S_5, $LiSC_2H_5$	THF	140	0.132	42
$Li_7P_3S_{11}$	Li_2S, P_2S_5	ACN	220	1.5	55-56
$Li_7P_3S_{11}$	Li_2S, P_2S_5	DME	250	0.27	47
$Li_7P_3S_{11}$	Li_2S, P_2S_5	ACN	250	0.97	48
$Li_7P_3S_{11}$	Li_2S, P_2S_5	ACN	260	1.5	49
$Li_7P_2S_8I$	Li_2S, P_2S_5, LiI	EP	170	0.46	41
$Li_7P_2S_8I$	Li_2S, P_2S_5, LiI	ACN	200	0.63	46
Li_4PS_4I	Li_2S, P_2S_5, LiI	DME	200	0.12	52

DME, 1,2-dimethoxyethane; THF, tetrahydrofuran; ACN acetonitrile; EA, ethyl acetate; EP, ethyl propionate. *a-Li_3PS_4: amorphous-Li_3PS_4

The preparation of highly lithium-ion conductive $Li_7P_3S_{11}$ phase (FIG. **2c**) using DME was reported by Machida et al. in 2014.[47] The process included the stirring of starting materials in DME for 72 hours and subsequent heating at different temperatures. X-ray diffraction (XRD) patterns showed the formation of $Li_7P_3S_{11}$ phase and Raman spectra of the products heated at 200 and 250 °C showed peaks at 420 and 405 cm^{-1} corresponding to the PS_4^{3-} and $P_2S_7^{4-}$ units, respectively (FIG. **2d**). $Li_7P_3S_{11}$ phase decomposed at 300 °C and exhibited a maximum ionic conductivity 2.7×10^{-4} S cm^{-1} at room temperature.[47]

From 2015, more studies reported on electrolytes exhibiting ionic conductivities close to 10^{-3} S cm^{-1} that were attained through mixing of starting materials in a solvent for 24–72 hours. $Li_7P_3S_{11}$ electrolyte was prepared using ACN, ACN–THF, and THF, and the maximum ionic conductivity of 9.7×10^{-4} S cm^{-1} at 25 °C was found in the product synthesized using ACN and heated at 250 °C.[48] Another study showed that higher conductivities up to 1.5×10^{-3} S cm^{-1} at room temperature could be attained if $Li_7P_3S_{11}$ was instead heated at 260 °C.[49] Liu et al. proposed a two-step mechanism for the synthesis of $Li_7P_3S_{11}$ using ACN and heat.[43] First, Li_3PS_4·ACN complex in solution dissolving Li_2S·P_2S_5 were formed, and heat produce the mixture of Li_3PS_4·ACN and Li_2S·P_2S_5. Subsequent solid-state reaction between the two resulted in the formation of $Li_7P_3S_{11}$. The ionic conductivity after heating at 260 °C was 8.7×10^{-4} S cm^{-1}. β-Li_3PS_4 was synthesized using either EA[50] or ACN[51], achieving conductivities of 3.3×10^{-4} and 1.2×10^{-4} S cm^{-1}, respectively. Li_4PS_4I was synthesized first by mixing Li_3PS_4·DME complex and LiI in DME to form Li_3PS_4·DME·LiI complex and then heating the intermediates at 50-200 °C.[52] The ionic conductivity was determined to be in the range of 6.4×10^{-5} –1.2×10^{-4} S cm^{-1} at room temperature.

Enhancement of the kinetics of suspension reactions to shorten synthesis time has been achieved by using various mixing approaches. For example, the use of zirconia balls to shake the mixture of Li_2S and P_2S_5 in DMC[53] facilitated the formation of amorphous Li_3PS_4 (conductivity, 6×10^{-6} S cm^{-1}) and Li_3PS_4–LiI solid solutions in the presence of LiI and EP (conductivity, 3.4×10^{-4} S cm^{-1}).[54] The typical mixing time was 1.5–6 h, which was significantly shorter than those reported above. $Li_7P_3S_{11}$ (conductivities, 0.9–1.5×10^{-3} S cm^{-1}) was synthesized in ACN performing ultrasonification for one hour followed by a heat treatment at 220 °C.[55-56]Another approach to increase the kinetics is to use a homogeneous solution as intermediate.[41] The reaction between P_2S_5 and LiI was completed without solid precipitates for a LiI:P_2S_5 molar ratio of 2. Li_2S was then added to this solution shortening the mixing time to 30–60 minutes . The following mechanism was proposed for the reaction between Li_2S, P_2S_5 and LiI in EP:

$$LiI + P_2S_5 \rightarrow LiI \cdot P_2S_5 \text{ (solution)} \quad (1)$$

$$LiI \cdot P_2S_5 \text{ (solution)} + 3\ Li_2S \rightarrow 2\ Li_3PS_4 \text{ complex} + LiI \quad (2)$$

β-Li_3PS_4 with an ionic conductivity of 1.32×10^{-4} S cm^{-1} was synthetized using the same approach with the addition of a nucleophilic agent, $LiSC_2H_5$, and a mixing time of 12 hours.[42]

To overview the trends of synthesis conditions in suspension synthesis, the ionic conductivities of electrolytes near room temperature prepared are plotted against the maximum heating temperatures (FIG. **2e**).Ionic conductivities presented in this review are mostly measured using alternating current (AC) impedance measurements under an inert atmosphere. Some previous research confirmed the ionic transport number to be unity using additional direct current (DC) measurements of Li/electrolyte/Li cell.[50, 54, 57] The range of synthesis temperatures is 80–300 °C and the maximum ionic conductivity of electrolytes is 1.5×10^{-3} S cm^{-1}. Because suspension approaches require lower temperatures compared to those required in solid-state syntheses (typically above 500 °C), metastable phases such as β-Li_3PS_4 and $Li_7P_3S_{11}$, have been observed. New phases in Li_2S–P_2S_5–LiI were attained as a result of such suspension syntheses, suggesting that this approach could be used to explore new material(s). The synthesized powders were submicron to a few microns in size[44, 55-56, 58] and exhibited highly porous structures,[44] which were favorable for producing dense membranes by cold- or warm-sintering[46, 55, 59]. Although, the ionic conductivity of β-Li_3PS_4 synthesized using suspension approaches is approximately three-orders of magnitude higher than that achieved by solid-state synthesis,[44] the conductivities of other phases are lower than those achieved by solid-state syntheses. The broad range of conductivity of electrolytes attained through liquid-phase syntheses suggests that optimization of synthesis conditions is necessary to achieve electrolytes with high conductivities.

Overall, an advantage of the suspension synthesis is that highly lithium conductive and metastable solid electrolytes are synthesized from commercially available Li_2S and P_2S_5. Knowledge of both kinetic and thermodynamic of the formation and decomposition of complexes is necessary to understand the reaction mechanism of metastable phases. An accurate structural analysis of complexes and products can enable further understanding. We believe that this method has the potential to produce new sulfide electrolytes that cannot be obtained by other approaches. In addition, the conductivity of some of the synthesized electrolytes through this method is greater than 1×10^{-3} S cm^{-1}, which makes these electrolytes suitable for use in all-solid-state batteries.

2-2. Dissolution–Precipitation

In addition to suspension syntheses, dissolution–precipitation approaches in which a solid electrolyte is completely dissolved in a homogeneous solution have been reported (Table 2, FIG. **3a**). Generally, solid electrolytes attained by solid-state synthesis or ball milling are first dissolved in organic solvents such as hydrazine, N-methylformamide (NMF), methanol, and ethanol in which they are highly soluble. Then, the solvent is removed by evaporation and leaving the solid product, the phases of which is usually the same as that before dissolution. Handling of the electrolyte is usually performed in an Ar glove box or under vacuum to prevent the exposure to air and water. Homogeneous solutions (FIG. **3b**) are suitable for producing thin layers after evaporation of solvent.

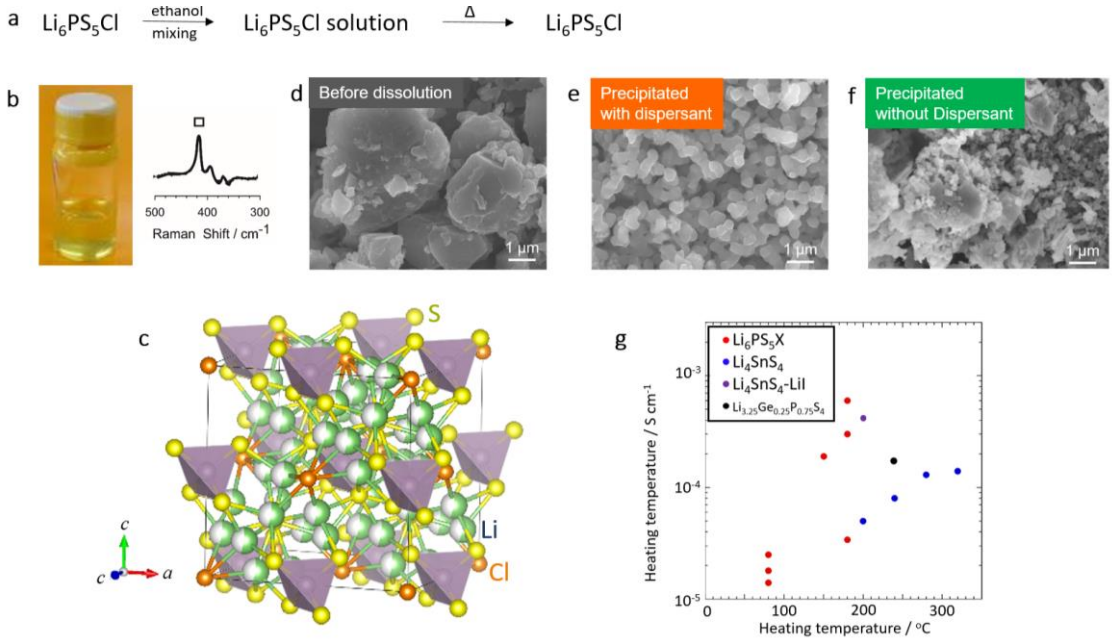

Figure 3. Dissolution‑precipitation of sulfide electrolyte. **a** Dissolutionprecipitation reaction for the synthesis of representative sulfide-based solid electrolyte. **b** Picture of Li_6PS_5Cl‑ethanol solution and the corresponding Raman spectrum showing PS_4^{3-}.[62] PS_4^{3-} unit dissolved in ethanol is stable and can be precipitated by removing solvent. **c** Crystal structure of Li_6PS_5Cl with tetrahedrons being PS_4^{3-}.[16, 79] **d** Irregular-shaped Li_6PS_5Cl particles synthesized by high-energy ball-milling process.[65] **e** Homogeneous and submicron-sized Li_6PS_5Cl particles precipitated from a Li_6PS_5Cl‑etanol solution with dispersant.[65] **f** Irregular-shaped Li_6PS_5Cl particles precipitated from a Li_6PS_5Cl‑etanol solution without dispersant.[65] **g** Heating temperatures of dissolution-precipitation processes and corresponding conductivities (near room temperature) of precipitated electrolytes. [28-29, 57, 62-64, 66]

TABLE 2 Dissolution-precipitation of sulfide-based solid electrolytes and conductivities near room temperature.

Product	Synthesis	Solvent	Temp. (°C)	σ (mS cm^{-1})	Ref.
LGPS	SS	Hydrazine	240	0.113	57
Li_2S·P_2S_5	BM	NMF	150	0.0026	60
Li_6PS_5Cl	BM	Ethanol	80	0.014	62
Li_6PS_5Cl	BM	Ethanol	150	0.19	64
Li_6PS_5Cl	BM	ACN-Ethanol	180	0.6	65
Li_6PS_5Br	SP	EP-Ethanol	180	0.034	66
Li_4SnS_4	SS	Methanol	200	0.09	28
Li_4SnS_4	SS	Water	320	0.14	3030
0.6Li_4SnS_4 ·0.4LiI	SS	Methanol	200	0.41	28

LGPS: $Li_{3.25}Ge_{0.25}P_{0.75}S_4$, SP: Suspension synthesis, SS: Solid-state synthesis, BM: ball-milling synthesis; NMF. N-methylformamide; ACN acetonitrile; EP, ethyl propionate.

In 2012, Huang and co-workers reported the dissolution–precipitation of $Li_{3.25}Ge_{0.25}P_{0.75}S_4$ dissolved in anhydrous hydrazine as solvent.[57] Subsequent heating in dry nitrogen at 240 °C produced powder and thin film of $Li_{3.25}Ge_{0.25}P_{0.75}S_4$. The lithium-ion conductivities of powder and thin film at 30 °C were 1.1×10^{-4} and 1.8×10^{-4} S cm^{-1}, respectively. Hayashi, Tatsumisago and co-workers produced Li_2S–P_2S_5 solid electrolyte using NMF as solvent.[60] Dissolving $80Li_2S \cdot 20P_2S_5$ glass synthesized by ball milling in NMF produced a yellow solution and further heating at 150 °C under vacuum led to Li_2S–P_2S_5 solid electrolyte with ionic conductivity of 2.6×10^{-6} S cm^{-1} at 25 °C. Instead, Li_3PS_3 with conductivity of 2.3×10^{-6} S cm^{-1} was fist dissolved in NMF and then precipitated after the solution was heated at 180 °C.[61]

Argyrodites, such as Li_6PS_5Cl, consist of Li^+, PS_4^{3-} and monovalent anions are attractive sulfide electrolytes because of their high Li^+ conductivity of 10^{-2}–10^{-3} S cm^{-1} at room temperature.[16] Li_6PS_5Cl–ethanol solution was attained by dissolving Li_6PS_5Cl synthesized by ball-milling in anhydrous ethanol. Raman spectra of the transparent ethanol solution clearly revealed the presence of PS_4^{3-} ions(FIG. **3b**).[62] After heating to evaporate solvent, Li_6PS_5Cl phase exhibiting PS_4^{3-} unit was precipitated (FIG. **3c**).[62-65] The conductivities of the dried product at 80 °C and 150 °C were 1.4×10^{-5} S cm^{-1} (Ref.[62]) and 1.9×10^{-4} S cm^{-1} (Ref.[64]), respectively. Before dissolution, particles of Li_6PS_5Cl synthesized by high-energy ball milling were irregular in shape (FIG. **3d**). The heating at 180 °C and the addition of dispersant in mixture of acetonitrile and ethanol helped achieving homogeneous and submicron-sized Li_6PS_5Cl particles (FIG. **3e**) [65], whereas aggregates of a few microns in size were attained without the addition of the dispersant (FIG. **3f**). The conductivities of the electrolyte synthesized with and without dispersant reached 6×10^{-4} and 3×10^{-4} S cm^{-1}, respectively. Isostructural argyrodites, Li_6PS_5X (X = Cl, Br, and I), were also synthesized using ethanol, which was evaporated by heating at 80 or 150 °C. The conductivities of these precipitates were in the range 10^{-5} to 10^{-4} S cm^{-1}. [64]

Li_4SnS_4 and their derivatives are attractive because of their high stability in water. Jung and co-workers reported on LiI–Li_4SnS_4 dissolved in methanol[28] and water.[29] Li_4SnS_4 synthesized by solid-state synthesis was dissolved in methanol (with LiI) or deionized water (without LiI), releasing in both cases negligible quantity of H_2S. The high stability of the SnS_4^{4-} in water could be explained by the lower affinity of O^{2-} for Sn^{4+} than for P^{5+}. The precipitates from methanol at 200 °C exhibited an amorphous phase and a maximum conductivity 4.1×10^{-4} S cm^{-1}.[28] The precipitates from the aqueous solution heated at and above 320 °C were indexed as Li_4SnS_4 and their maximum conductivity was 1.4×10^{-4} S cm^{-1}.[29]

A combined approach of suspension synthesis and subsequent dissolution–precipitation was proposed for the solution synthesis using Li_2S and P_2S_5 as starting materials.[66-67] In the first step, the mixing of Li_2S, P_2S_5 and LiBr powders in EP or THF led to an electrolyte suspension of PS_4^{3-} complexes. The addition of ethanol to this suspension produced a transparent solution, and subsequent heating at 180 °C precipitated Li_6PS_5Br powder with conductivity 3.4×10^{-5} S cm^{-1}.[66] The conductivity of the precipitated electrolyte sintered at 550 °C reached 3.1×10^{-3} S cm^{-1};[67] the sintering temperature and conductivity were comparable to those prepared by solid-state reaction.[16]

The ionic conductivities near room temperature of electrolytes prepared by dissolution–precipitation are plotted against the maximum heating temperature (FIG. **3g**). Most heating temperatures are between 80 and 320 °C and the conductivities of electrolytes in this temperature range are below 1×10^{-3} S cm^{-1}. Most of the synthesized phases are thermodynamically stable in contrast to those obtained by suspension synthesis. The phases of the precipitated solid electrolytes were the same as those before being dissolved, but the conductivities of precipitated electrolytes were not as high as those before dissolution. For instance, argyrodites most of Li_6PS_5X synthesized by dissolution–precipitation and heating below 300 °C showed 10^{-5}–10^{-4} S cm^{-1}, which are at least one order lower than those synthesized by solid-state reaction (~10^{-3} S cm^{-1}) (Ref.[17]). The use of water in Li_4SnS_4 was advantageous in reducing the environmental cost, but in most cases higher heating temperatures were needed to remove the solvents.

One of the advantages of the dissolution–precipitation process is that it affords homogeneous solid electrolytes derived from a homogeneous solution. Therefore, this approach is preferred for the syntheses of electrolytes for composite electrodes because the homogeneous solution penetrates electrode particles with relative ease. Additionally, particle size and shape of precipitates can be controlled through removal of solvents and surface modification based on nucleation and crystal growth in homogeneous solution. Although significant advancements have been made in regard to the dissolution–precipitation process using different solvents, reducing the heating temperature while completely removing organic solvent and maintaining high conductivity continues to be a challenge; as it stands, no study has been published reporting a conductivity higher than 1×10^{-3} S cm^{-1} achieved with a heating temperature below 300 °C.

3. Liquid-phase processes for electrode composites

In this section, we introduce the liquid-phase processes used to prepare composite electrodes. In these processes, electrodes and additives are first immersed in suspensions or solutions of solid electrolytes (or their precursors), then the evaporation of the solvent leads to the formation of the electrode–electrolyte composite particles (Fig. **4a**). Liquid-phase processes lead to electrolyte layers on electrodes, minimizing the amount of solid electrolyte and thus enhancing the energy density of all-solid-state batteries.

Also for the production of electrode composites we categorize the liquid-phase processes into suspension and dissolution–precipitation processes. Tables 3 shows the conditions tested for the preparation of composite electrodes using liquid-phase processes and the capacities of the cells including the composites.

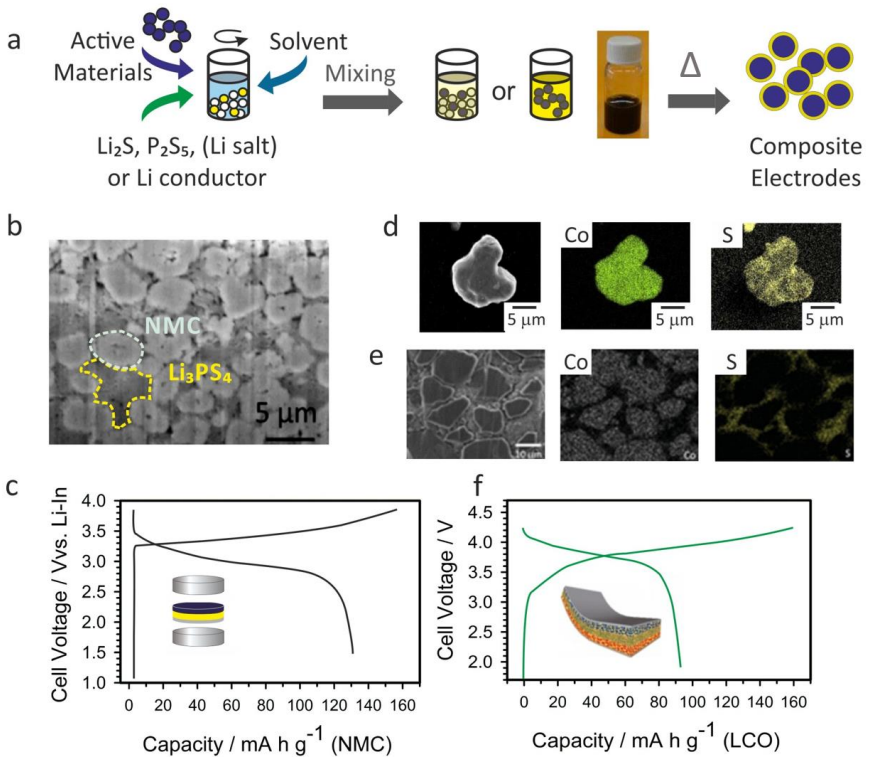

Figure 4 Liquid-phase processes for composite electrodes of all-solid-state lithium batteries. **a** Scheme of liquid-phase process of composite electrodes. **b** Cross-section image of composite electrodes of $LiNi_{1/3}Co_{1/3}Mn_{1/3}O_2$ and Li_3PS_4 prepared by suspension synthesis.[68] **c** First charge-discharge curve of bulk-type all-solid-state battery using the positive electrode composite of $LiNi_{1/3}Co_{1/3}Mn_{1/3}O_2$ and Li_3PS_4 prepared by suspension synthesis; Li-In alloy is used as a negative electrode.[68] **d** Scanning electron microscopy and energy dispersive X-ray analysis mapping (Co and S) images of a $LiCoO_2$ particle coated with Li_6PS_5Cl solid electrolyte precipitated from Li_6PS_5Cl-ethanol solution. [62] **e** Scanning electron microscopy and energy dispersive X-ray analysis mapping (Co and S) images of composite of $LiCoO_2$ and Li_6PS_5Cl precipitated from Li_6PS_5Cl-ethanol solution.[73] **f** Charge-discharge curves of sheet-type all-solid-state battery fabricated by dissolution-precipitation process; active materials of positive and negative electrodes are $LiCoO_2$ and graphite, respectively, and Li_6PS_5Cl-ethanol solution is used as electrolyte.[73]

TABLE 3 Synthesis conditions of composite electrodes prepared by suspension synthesis and their capacities.

Electrolyte	wt%	Active material	wt%	Others	wt%	Solvent	Temp.(°C)	Capacity*** (mA h g^{-1})	Ref.
				Suspension Synthesis					
Li_3PS_4	10	NCM_{111}	90	-		EP	170	130 (BT)	68
$Li_7P_3S_{11}$	50*	Co_9S_8	40**	Super P	10	ACN	260	650 (BT)	49
$Li_7P_3S_{11}$	50*	Fe_3S_4	45**	Super P	5	ACN	260	1001 (BT)	70
$Li_7P_3S_{11}$	60*	MoS_2	30**	AB	10	ACN	250	700 (BT)	71
Li_3PS_4	27.5	NCM_{622}	70	Super C65 NBR	1 1.5	THF	140	150 (ST)	69
Li_3PS_4	47.5	Graphite	50	NBR	1.5	THF	140	320 (ST)	69
				Dissolution-Precipitation					
Li_3PS_4	7.5	$LiCoO_2$	92.5	-		NMF	180	32 (BT)	61
Li_6PS_5Cl	7.5	$LiCoO_2$	92.5	-		Ethanol	80	45 (BT)	62
Li_4SnS_4·LiI	15	$LiCoO_2$	85	-		Methanol	200	135 (BT)	28
Li_4SnS_4	15	$LiCoO_2$	85	-		Water	320	130 (BT)	29
Li_6PS_5Cl	14	NCM_{111}	84	VGCF	2	Ethanol	80	44 (BT)	63

Li_6PS_5Cl	3	$LiCoO_2$	97	Super P PVDF	2 1	Ethanol	180	150 (ST)	73
Li_6PS_5Cl	5	Graphite	95	PVDF	5	Ethanol	180	320 (ST)	73
Li_6PS_5Br	14	NCM_{111}	84	VGCF	2	EP +Ethanol	180	109 (BT)	66
Li_6PS_5Cl	14	NCM_{111}	84	VGCF	2	EA +Ethanol	150	160 (BT)	72
Li_6PS_5Cl	9	NCM_{111}	89	VGCF Triton	2 0.1	ACN +Ethanol	150	115 (BT)	65
Li_6PS_5Br	10	NCM_{111}	90	-	-	THF + Ethanol	150	120(BT)	67

AB: acetylene carbon black, Super P, and Super C65 as carbon additives, NBR: nitrile-butadiene rubber as binder; VGCF: vapor-grown carbon fiber, PVDF: polyvinylidene difluoride, NCM_{111}, $LiNi1_{/3}$ $Co_{1/3}Mn_{1/3}O_2$; NCM_{622}, $LiNi_{0.6}$ $Co_{0.2}Mn_{0.2}O_2$; ACN, acetonitrile; EA, ethyl acetate; EP, ethyl propionate; THF, tetrahydrofuran (BT): bulk-type and (ST) and sheet-type ASLB cells. *added by hand-milling mixture to produce composite. ** including the content of $Li_7P_3S_{11}$-layer.*** capacity per weight of active material.

3-1. Suspension syntheses

Suspension syntheses are processes in which electrodes and additives are mixed in suspensions of solid electrolytes (or their precursors), usually, synthesized from Li_2S and P_2S_5. After evaporation of the solvent, a composite electrode containing active material that features Li ion and electron paths is obtained. To maximize the energy density of all-solid-state batteries, minimum amounts of solid electrolytes that sustain lithium conduction pathway should be used.

Phuc, Matsuda and co-workers used suspension synthesis to prepare Li_3PS_4 (conductivity, 2×10^{-4} S cm^{-1} at room temperature) from Li_2S and P_2S_5 in EP with zirconium balls to achieve a fast mixing. A suspension for a positive composite electrode was then prepared by adding 90 wt% $LiNi_{1/3}Co_{1/3}Mn_{1/3}O_2$, so called NCM111, as active material.[68] This suspension was heated at 170 °C for 2 hours under vacuum. The active material particles were well dispersed in the solid electrolyte matrix for the composite electrode (Fig. **4b**), resulting in a high initial discharge capacity of up to 130 mA h g^{-1} in bulk-type all-solid-state batteries (Fig. **4c**).

Li_3PS_4–THF suspension has also been used to prepare sheet-type all-solid-state batteries. A solid electrolyte layer was added on $LiNi_{0.6}Co_{0.2}Mn_{0.2}O_2$, NCM622, and graphite electrodes.[69] Polymeric binders such as nitrile-butadiene rubber (NBR) or polyvinyl chloride (PVC) compatible with THF were used to improve the adhesion and mechanical properties of the positive composite electrode. Although there were cracks in the composite electrodes, both the electrodes displayed high initial discharges of 150 and 320 mA h g^{-1} for NCM622 and graphite, respectively. In addition, a full sheet-type all-solid-state battery showed high discharge capacity and capacity retention of 120 mA h g^{-1} at 30 and 100 °C.

The high ionic conductor $Li_7P_3S_{11}$ was used to prepare a buffer layer for sulfide-type electrodes such as Co_9S_8, Fe_3S_4, and MoS_2 to achieve close contact with the additional $Li_7P_3S_{11}$ solid electrolyte. Sulfide-type electrodes coated with $Li_7P_3S_{11}$ were mixed with additional $Li_7P_3S_{11}$ powders by hand milling. Compared to uncoated electrode, bulk-type all-solid-state batteries featuring $Li_7P_3S_{11}$-layer showed improved charge and discharge capacities higher than 600 mA h g^{-1}.[49, 70-71]

3-2. Dissolution–Precipitation

Homogeneity of composite materials is important, therefore the dissolution-reprecipitation process using a homogenous solution would be critical to the fabrication of composite materials for positive and negative electrodes. The liquid precursor of sulfide electrolyte can easily cover the surface of the electrode particles. After removing solvent, homogeneous composites, which are difficult to obtain by a simple mixture procedure of the particles of electrode and solid electrolyte, can be formed.

$LiCoO_2$ particles were coated with $80Li_2S{\cdot}20P_2S_5$[61] and Li_6PS_5Cl[62] dissolved in N-methyl formamide and ethanol, respectively. The coating of a solid electrolyte layer on $LiCoO_2$ particles was verified by scanning electron microscopy and energy dispersive X-ray analyses (Fig. **4d)**. Bulk-type all-solid-state batteries constructed with coated particles exhibited better charge–discharge capacity than uncoated positive electrode, with the former achieving 30–50 mA h g^{-1} [61-62]. Several mixtures of protic and aprotic solvents helped producing a layer of solid electrolyte on $LiNi_{1/3}Co_{1/3}Mn_{1/3}O_2$ that promoted a better interface between the active material and solid electrolyte in a bulk-type all-solid-state battery.[63, 65, 72] For example, a combination of ethyl acetate and ethanol led to a very high initial discharge capacity of 160 mA h g^{-1} in a composite electrode prepared with 14 wt% layer of solid electrolyte. Bulk-type all-solid-state batteries fabricated with composite positive electrodes derived from liquid-phase processes containing dispersants show high initial discharge capacities of 110 mA h g^{-1}, better than those attained without the use of dispersants (40 mA h g^{-1}).[65] Infiltration of Li_6PS_5Cl-solution into tortuous porous structures of sheet-type electrodes produced adequate ionic conduction pathways, providing intimate ionic contacts and favorable ionic percolation (Fig. **4e**).[73] The capacity of a full sheet-type all-solid lithium battery was ~ 100 mA h g^{-1} (Fig. **4f**).

Electrolyte solutions of 0.4 LiI-0.6 Li_4SnS_4 and Li_4SnS_4 using methanol and water as solvents, respectively, were produced and used with $LiCoO_2$ for the preparation of composite electrodes. [28-29] Bulk-type all-solid-state batteries fabricated with these positive composite

electrodes (15 wt% solid electrolyte) achieved good electrochemical performances as testified by high initial discharge capacities of 135 mA h g^{-1}.

Summary and Outlook

With the recent increased attention on sulfide-based all-solid-state lithium batteries, liquid-phase approaches for the production of sulfide electrolytes have assumed greater importance. In the past years, significant advancements have been made concerning reactions for the synthesis of sulfide electrolytes and the preparation of composites used in all-solid-state lithium batteries. All-solid-state batteries using different solid electrolytes for negative electrodes, electrolyte layer and positive electrodes can be now designed. This flexible design, however, requires the use of a variety of electrolytes and synthesis approaches to achieve the specific requirements of each of the components of all-solid-state batteries. For example, given that ion conductivity for a solid electrolyte layer often needs to be in the range 10^{-3}-10^{-2} S cm^{-1}, suspension synthesis for producing a high-conductive phase would be suitable for such an electrolyte layer. On the other hand, for composite electrodes, dissolution–precipitation processes provide the advantage of producing homogeneously distributed electrode and electrolyte as well as a large interfacial contact between them; however, scope for improvement remains in the conductivity of precipitated electrolyte achieved with such processes. The requisite electrochemical window for electrolytes for positive electrodes is in the high-potential range, typically 3–5 V vs. Li/Li^+, whereas that for negative electrodes is in the low-potential range, typically 0–1 V vs. Li/Li^+. Suppressing Li dendrite formation is essential for the use of lithium metal as a negative electrode. Also, combining sulfide electrolytes with other electrolytes, such as oxides and halides, expands the flexibility of design. Evidently, solution chemistry needs to be further enriched in order to optimize the configurations and fabrication processes of all-solid-state batteries.

In this Review, we categorize liquid-phase reactions into suspension syntheses for the production of sulfide electrolytes typically from Li_2S and P_2S_5, and dissolution–precipitation using solid electrolytes synthesized typically by solid-state synthesis or the ball-milling process. Suspension syntheses involve the mixing of starting precursors in organic solvents to form complexes, and their thermal decomposition to produce nanoporous sulfide-electrolytes. An increase in reaction kinetics was achieved by modifying the mixing methods, such as shaking with zirconium balls and ultrasonification, and by using highly soluble intermediates. The synthesized phases are often thermodynamically metastable and include $Li_7P_3S_{11}$ with conductivity above 1×10^{-3} S cm^{-1}. Newly discovered compounds in the Li–P–S–I system expand the chemical space useful for sulfide-based electrolytes. Dissolution–precipitation uses highly-polar solvents such as ethanol. The stability of the P–S unit in such solutions enables the precipitation of solid electrolytes from organic solvents. In most reported cases, the crystal structures of precipitates are thermodynamically stable phases.

Both suspension reaction and dissolution–precipitation are utilized in producing composite electrodes for all-solid-state batteries. They are scalable as they include the mixing of electrodes, electrolyte, and electron conductors without the use of special apparatuses. Composites produced with electrolyte less than 10 wt% show discharge capacity above 100 mA h g^{-1}. Liquid-phase reactions are also used for the production of Na ion conductors,[74-76] and applied in all-solid-state sodium batteries.[77] For lithium batteries that use organic electrolytes, the negative composite electrode coated with $Li_7P_3S_{11}$ was also prepared in this suspension reaction.[78]

Liquid-phase chemistry concerning sulfide electrolytes is growing rapidly and synthesized composite electrodes are being used in sulfide-based all-solid-state lithium batteries. Liquid-phase chemistry offers a synthesis tool to optimize properties of solid electrolytes by controlling chemical reactions through the use of starting materials and synthesis protocols. However, many challenges still remain. The synthesis mechanism based on a suspension of starting materials to produce sulfide-electrolytes has not yet been clarified and the conductivities of most electrolytes prepared using liquid-phase processes are not as high as those prepared by solid-state reactions. Further efforts are required to lower the temperatures to completely remove organic solvent. This development is important to simplify the process and avoid undesirable reactions in composites. Manufacturing the sheet electrolyte and composite electrodes devoid of cracks is important for all-solid-state batteries. In order to scale up for industrial application, a process carried out using dry air with a dew point of -40 to -20 °C needs to be established. Nonetheless, we believe that sulfide liquid-phase chemistry has made big leaps in the last years and has the potential to be extended not only into manufacture of all-solid-state lithium batteries and other chalcogenides but also into other applications.

AUTHOR INFORMATION

Corresponding Authors

*Kiyoharu Tadanaga: tadanaga@eng.hokudai.ac.jp
*Masahiro Tatsumisago: tatsu@chem.osakafu-u.ac.jp

Notes

The authors declare no financial and/or non-financial interest.

Contributions

AM, NCRN, AS and KT wrote the draft. NHHP, AM, NM, AH, and MT discussed with the review. All the authors agreed the final version of manuscript.

ACKNOWLEDGMENT

This review includes the research achievements partially supported by the Japan Science and Technology Agency (JST), the Advanced Low Carbon Technology Research and Development Program (ALCA), and the Specially Promoted Research for Innovative Next Generation Batteries (SPRING) project.

REFERENCES

1. Tatsumisago, M.; Nagao, M.; Hayashi, A., Recent development of sulfide solid electrolytes and interfacial modification for all-solid-state rechargeable lithium batteries. *J. Asian Ceram. Soc.* **2013,** *1* (1), 17-25.
2. Hayashi, A.; Sakuda, A.; Tatsumisago, M., Development of Sulfide Solid Electrolytes and Interface Formation Processes for Bulk-Type All-Solid-State Li and Na Batteries. *Front. Energy Res.* **2016,** *4*.
3. Manthiram, A.; Yu, X.; Wang, S., Lithium battery chemistries enabled by solid-state electrolytes. *Nat. Rev. Mater.* **2017,** *2* (4).
4. Gao, Z.; Sun, H.; Fu, L.; Ye, F.; Zhang, Y.; Luo, W.; Huang, Y., Promises, Challenges, and Recent Progress of Inorganic Solid-State Electrolytes for All-Solid-State Lithium Batteries. *Adv. Mater.* **2018**.
5. Park, K. H.; Bai, Q.; Kim, D. H.; Oh, D. Y.; Zhu, Y.; Mo, Y.; Jung, Y. S., Design Strategies, Practical Considerations, and New Solution Processes of Sulfide Solid Electrolytes for All-Solid-State Batteries. *Adv. Energy Mater.* **2018**, 1800035.
6. Meesala, Y.; Jena, A.; Chang, H.; Liu, R.-S., Recent Advancements in Li-Ion Conductors for All-Solid-State Li-Ion Batteries. *Adv. Mater. Interfaces* **2017,** *2* (12), 2734-2751.
7. Zheng, F.; Kotobuki, M.; Song, S.; Lai, M. O.; Lu, L., Review on solid electrolytes for all-solid-state lithium-ion batteries. *J. Power Sources* **2018,** *389*, 198-213.
8. Lim, H.-D.; Lim, H.-K.; Xing, X.; Lee, B.-S.; Liu, H.; Coaty, C.; Kim, H.; Liu, P., Solid Electrolyte Layers by Solution Deposition. *Adv. Mater. Interfaces* **2018,** *5* (8), 1701328.
9. Takada, K., Progress in solid electrolytes toward realizing solid-state lithium batteries. *J. Power Sources* **2018,** *394*, 74-85.
10. Hayashi, A.; Hama, S.; Morimoto, H.; Tatsumisago, M.; Minami, T., Preparation of Li_2S–P_2S_5 Amorphous Solid Electrolytes by Mechanical Milling. *J. Am. Ceram. Soc.* **2001,** *84* (2), 477-79.
11. Hayashi, A.; Hama, S.; Minami, T.; Tatsumisago, M., Formation of superionic crystals from mechanically milled Li_2S–P_2S_5 glasses. *Electrochem. Commun.* **2003,** *5* (2), 111-114.
12. Mizuno, F.; Hayashi, A.; Tadanaga, K.; Tatsumisago, M., New, Highly Ion-Conductive Crystals Precipitated from Li_2S–P_2S_5 Glasses. *Adv. Mater.* **2005,** *17* (7), 918-921.
13. Hong, H. Y.-P., Crystal structure and ionic conductivity of $Li_{14}Zn(GeO_4)_4$ and other new Li^+ superionic conductors. *Mater. Res. Bull.* **1978,** *13*, 117-124.
14. Kanno, R.; Murayama, M., Lithium ionic conductor thio-LISICON the Li_2S-GeS_2-P_2S_5 system. *J. Electrochem. Soc.* **2001,** *148*, A743-A746.
15. Kamaya, N.; Homma, K.; Yamakawa, Y.; Hirayama, M.; Kanno, R.; Yonemura, M.; Kamiyama, T.; Kato, Y.; Hama, S.; Kawamoto, K.; Mitsui, A., A lithium superionic conductor. *Nat Mater* **2011,** *10* (9), 682-6.
16. Deiseroth, H.-J.; Kong, S.-T.; Eckert, H.; Vannahme, J.; Reiner, C.; Zaiß, T.; Schlosser, M., Li_6PS_5X: A Class of Crystalline Li-Rich Solids With an Unusually High Li^+ Mobility. *Angew. Chem.* **2008,** *120* (4), 767-770.
17. Boulineau, S.; Courty, M.; Tarascon, J.-M.; Viallet, V., Mechanochemical synthesis of Li-argyrodite Li_6PS_5X (X=Cl, Br, I) as sulfur-based solid electrolytes for all solid state batteries application. *Solid State Ionics* **2012,** *221*, 1-5.
18. Inaguma, Y.; Liquan, C.; Itoh, M.; Nakamura, T.; Uchida, T.; Ikuta, H.; Wakihara, M., High ionic conductivity in lithium lanthanum titanate. *Solid State Commun.* **1993,** *86* (10), 689-693.
19. Aono, H.; Sugimoto, E.; Sadaoka, Y.; Imanaka, N.; Adachi, G. y., Ionic Conductivity of the Lithium Titanium Phosphate $(Li_{1+X}M_XTi_{2-X}(PO_4)_3$, M =Al, Sc, Y , and La) Systems. *J. Electrochem. Soc.* **1989,** *136* (2), 590-591.
20. Murugan, R.; Thangadurai, V.; Weppner, W., Fast lithium ion conduction in garnet-type $Li_7La_3Zr_2O_{12}$. *Angew. Chem.* **2007,** *46* (41), 7778-81.
21. Tadanaga, K.; Takano, R.; Ichinose, T.; Mori, S.; Hayashi, A.; Tatsumisago, M., Low temperature synthesis of highly ion conductive $Li_7La_3Zr_2O_{12}$–Li_3BO_3 composites. *Electrochem. Commun.* **2013,** *33*, 51-54.
22. Nagao, M.; Kitaura, H.; Hayashi, A.; Tatsumisago, M., High Rate Performance, Wide Temperature Operation and Long Cyclability of All-Solid-State Rechargeable Lithium Batteries Using Mo-S Chevrel-Phase Compound. *J. Electrochem. Soc.* **2013,** *160* (6), A819-A823.
23. Sakuda, A.; Hayashi, A.; Takigawa, Y.; Higashi, K.; Tatsumisago, M., Evaluation of elastic modulus of Li_2S-P_2S_5 glassy solid electrolyte by ultrasonic sound velocity measurement and compression test. *J. Ceram. Soc. Jpn.* **2013,** *121* (1419), 946-949.
24. Seino, Y.; Ota, T.; Takada, K.; Hayashi, A.; Tatsumisago, M., A sulphide lithium super ion conductor is superior to liquid ion conductors for use in rechargeable batteries. *Energy Environ. Sci.* **2014,** *7* (2), 627-631.
25. Sakuda, A.; Hayashi, A.; Tatsumisago, M., Sulfide solid electrolyte with favorable mechanical property for all-solid-state lithium battery. *Sci Rep* **2013,** *3*, 2261.
26. Ohta, N.; Takada, K.; Sakaguchi, I.; Zhang, L.; Ma, R.; Fukuda, K.; Osada, M.; Sasaki, T., $LiNbO_3$-coated $LiCoO_2$ as cathode material for all solid-state lithium secondary batteries. *Electrochem. Commun.* **2007,** *9* (7), 1486-1490.
27. Hayashi, A.; Muramatsu, H.; Ohtomo, T.; Hama, S.; Tatsumisago, M., Improvement of chemical stability of Li_3PS_4 glass electrolytes by adding M_xO_y (M = Fe, Zn, and Bi) nanoparticles. *J. Mater. Chem. A* **2013,** *1* (21), 6320.
28. Park, K. H.; Oh, D. Y.; Choi, Y. E.; Nam, Y. J.; Han, L.; Kim, J.-Y.; Xin, H.; Lin, F.; Oh, S. M.; Jung, Y. S., Solution-Processable Glass LiI-Li_4SnS_4 Superionic Conductors for All-Solid-State Li-Ion Batteries. *Adv. Mater.* **2016,** *28* (9), 1874-1883.
29. Choi, Y. E.; Park, K. H.; Kim, D. H.; Oh, D. Y.; Kwak, H. R.; Lee, Y. G.; Jung, Y. S., Coatable Li_4SnS_4 Solid Electrolytes Prepared from Aqueous Solutions for All-Solid-State Lithium-Ion Batteries. *Chemsuschem* **2017,** *10* (12), 2605-2611.
30. Muramatsu, H.; Hayashi, A.; Ohtomo, T.; Hama, S.; Tatsumisago, M., Structural change of Li_2S–P_2S_5 sulfide solid electrolytes in the atmosphere. *Solid State Ionics* **2011,** *182* (1), 116-119.
31. Manna, L.; Scher, E. C.; Alivisatos, A. P., Synthesis of Soluble and Processable Rod-, Arrow-, Teardrop-, and Tetrapod-Shaped CdSe Nanocrystals. *J. Am. Chem. Soc.* **2000,** *122* (51), 12700-12706.

32. Peng, X., Mechanisms for the Shape‐Control and Shape‐Evolution of Colloidal Semiconductor Nanocrystals. *Adv. Mater.* **2003,** *15* (5), 459-463.
33. Henkel, G.; Krebs, B., Metallothioneins: Zinc, Cadmium, Mercury, and Copper Thiolates and Selenolates Mimicking Protein Active Site Features − Structural Aspects and Biological Implications. *Chem. Rev.* **2004,** *104* (2), 801-824.
34. Prouzet, E.; Ouvrard, G.; Brec, R.; Seguineau, P., Room temperature synthesis of pure amorphous nickel hexathiodiphosphate $Ni_2P_2S_6$. *Solid State Ionics* **1988,** *31* (1), 79-90.
35. Huang, Z.-L.; Zhao, J.-T.; Mi, J.-X.; Mao, S.-Y.; Zheng, L.-S., Room Temperature Solid State Synthesis and Characterization of a New Chromium Thiophosphate $Cr_4(P_2S_6)_3$. *J. Solid State Chem.* **1999,** *144* (2), 388-391.
36. Sakuda, A.; Kitaura, H.; Hayashi, A.; Tadanaga, K.; Tatsumisago, M., Improvement of high-rate performance of all-solid-state lithium secondary batteries using $LiCoO_2$ coated with Li_2O-SiO_2 glasses. *Electrochemical and Solid State Letters* **2008,** *11* (1), A1-A3.
37. Auvergniot, J.; Cassel, A.; Ledeuil, J. B.; Viallet, V.; Seznec, V.; Dedryvere, R., Interface Stability of Argyrodite Li_6PS_5Cl toward $LiCoO_2$, $LiNi_{1/3}Co_{1/3}Mn_{1/3}O_2$, and $LiMn_2O_4$ in Bulk All-Solid-State Batteries. *Chem. Mater.* **2017,** *29* (9), 3883-3890.
38. Sakuda, A.; Hayashi, A.; Hama, S.; Tatsumisago, M., Preparation of Highly Lithium‐Ion Conductive $80Li_2S \cdot 20P_2S_5$ Thin‐Film Electrolytes Using Pulsed Laser Deposition. *J. Am. Ceram. Soc.* **2010,** *93* (3), 765-768.
39. Sakuda, A.; Hayashi, A.; Ohtomo, T.; Hama, S.; Tatsumisago, M., All-solid-state lithium secondary batteries using $LiCoO_2$ particles with pulsed laser deposition coatings of Li_2S–P_2S_5 solid electrolytes. *J. Power Sources* **2011,** *196* (16), 6735-6741.
40. Ito, Y.; Otoyama, M.; Hayashi, A.; Ohtomo, T.; Tatsumisago, M., Electrochemical and structural evaluation for bulk-type all-solid-state batteries using Li_4GeS_4-Li_3PS_4 electrolyte coating on $LiCoO_2$ particles. *J. Power Sources* **2017,** *360*, 328-335.
41. Phuc, N. H. H.; Yamamoto, T.; Muto, H.; Matsuda, A., Fast synthesis of Li_2S–P_2S_5–LiI solid electrolyte precursors. *Inorg. Chem. Front.* **2017,** *4* (10), 1660-1664.
42. Lim, H.-D.; Yue, X.; Xing, X.; Petrova, V.; Gonzalez, M.; Liu, H.; liu, p., Designing solution chemistries for low-temperature synthesis of sulfide-based solid electrolytes. *J. Mater. Chem. A* **2018**.
43. Wang, Y.; Lu, D.; Bowden, M.; El Khoury, P. Z.; Han, K. S.; Deng, Z. D.; Xiao, J.; Zhang, J.-G.; Liu, J., Mechanism of Formation of $Li_7P_3S_{11}$ Solid Electrolytes through Liquid Phase Synthesis. *Chem. Mater.* **2018,** *30* (3), 990-997.
44. Liu, Z.; Fu, W.; Payzant, E. A.; Yu, X.; Wu, Z.; Dudney, N. J.; Kiggans, J.; Hong, K.; Rondinone, A. J.; Liang, C., Anomalous high ionic conductivity of nanoporous β-Li_3PS_4. *J. Am. Chem. Soc.* **2013,** *135* (3), 975-8.
45. Homma, K.; Yonemura, M.; Kobayashi, T.; Nagao, M.; Hirayama, M.; Kanno, R., Crystal structure and phase transitions of the lithium ionic conductor Li_3PS_4. *Solid State Ionics* **2011,** *182* (1), 53-58.
46. Rangasamy, E.; Liu, Z.; Gobet, M.; Pilar, K.; Sahu, G.; Zhou, W.; Wu, H.; Greenbaum, S.; Liang, C., An iodide-based $Li_7P_2S_8I$ superionic conductor. *J. Am. Chem. Soc.* **2015,** *137* (4), 1384.
47. Ito, S.; Nakakita, M.; Aihara, Y.; Uehara, T.; Machida, N., A synthesis of crystalline $Li_7P_3S_{11}$ solid electrolyte from 1,2-dimethoxyethane solvent. *J. Power Sources* **2014,** *271*, 342-345.
48. Xu, R. C.; Xia, X. H.; Yao, Z. J.; Wang, X. L.; Gu, C. D.; Tu, J. P., Preparation of $Li_7P_3S_{11}$ glass-ceramic electrolyte by dissolution-evaporation method for all-solid-state lithium ion batteries. *Electrochim. Acta* **2016,** *219*, 235-240.
49. Yao, X.; Liu, D.; Wang, C.; Long, P.; Peng, G.; Hu, Y.-S.; Li, H.; Chen, L.; Xu, X., High-Energy All-Solid-State Lithium Batteries with Ultralong Cycle Life. *Nano Lett.* **2016,** *16* (11), 7148-7154.
50. Phuc, N. H. H.; Totani, M.; Morikawa, K.; Muto, H.; Matsuda, A., Preparation of Li_3PS_4 solid electrolyte using ethyl acetate as synthetic medium. *Solid State Ionics* **2016,** *288*, 240-243.
51. Wang, H.; Hood, Z. D.; Xia, Y.; Liang, C., Fabrication of ultrathin solid electrolyte membranes of β-Li_3PS_4 nanoflakes by evaporation-induced self-assembly for all-solid-state batteries. *J. Mater. Chem. A* **2016,** *4* (21), 8091-8096.
52. Sedlmaier, S. J.; Indris, S.; Dietrich, C.; Yavuz, M.; Dräger, C.; von Seggern, F.; Sommer, H.; Janek, J., Li_4PS_4I: A Li+ Superionic Conductor Synthesized by a Solvent-Based Soft Chemistry Approach. *Chem. Mater.* **2017,** *29* (4), 1830-1835.
53. Phuc, N. H. H.; Morikawa, K.; Totani, M.; Muto, H.; Matsuda, A., Chemical synthesis of Li_3PS_4 precursor suspension by liquid-phase shaking. *Solid State Ionics* **2016,** *285*, 2-5.
54. Phuc, N. H. H.; Hirahara, E.; Morikawa, K.; Muto, H.; Matsuda, A., One-pot liquid phase synthesis of $(100-x)Li_3PS_4$–xLiI solid electrolytes. *J. Power Sources* **2017,** *365*, 7-11.
55. Calpa, M.; Rosero-Navarro, N. C.; Miura, A.; Tadanaga, K., Instantaneous preparation of high lithium-ion conducting sulfide solid electrolyte $Li_7P_3S_{11}$ by a liquid phase process. *RSC Adv.* **2017,** *7* (73), 46499-46504.
56. Calpa, M.; Rosero-Navarro, N. C.; Miura, A.; Tadanaga, K., Preparation of sulfide solid electrolytes in the Li_2S–P_2S_5 system by a liquid phase process. *Inorg. Chem. Front.* **2018,** *5* (2), 501-508.
57. Wang, Y.; Liu, Z.; Zhu, X.; Tang, Y.; Huang, F., Highly lithium-ion conductive thio-LISICON thin film processed by low-temperature solution method. *J. Power Sources* **2013,** *224*, 225-229.
58. Choi, S.; Lee, S.; Park, J.; Nichols, W. T.; Shin, D., Facile synthesis of Li_2S–P_2S_5 glass-ceramics electrolyte with micron range particles for all-solid-state batteries via a low-temperature solution technique (LTST). *Appl. Surf. Sci.* **2018,** *444*, 10-14.
59. Azuma, S.; Aiyama, K.; Kawamura, G.; Muto, H.; Mizushima, T.; Uchikoshi, T.; Matsuda, A., Colloidal processing of Li_2S–P_2S_5 films fabricated via electrophoretic deposition methods and their characterization as a solid electrolyte for all solid state lithium ion batteries. *J. Ceram. Soc. Jpn.* **2017,** *125* (4), 287-292.
60. Teragawa, S.; Aso, K.; Tadanaga, K.; Hayashi, A.; Tatsumisago, M., Preparation of Li_2S–P_2S_5 solid electrolyte from N-methylformamide solution and application for all-solid-state lithium battery. *J. Power Sources* **2014,** *248*, 939-942.
61. Teragawa, S.; Aso, K.; Tadanaga, K.; Hayashi, A.; Tatsumisago, M., Liquid-phase synthesis of a Li_3PS_4 solid electrolyte using *N*-methylformamide for all-solid-state lithium batteries. *J. Mater. Chem. A* **2014,** *2* (14), 5095-5099.
62. Yubuchi, S.; Teragawa, S.; Aso, K.; Tadanaga, K.; Hayashi, A.; Tatsumisago, M., Preparation of high lithium-ion conducting Li_6PS_5Cl solid electrolyte from ethanol solution for all-solid-state lithium batteries. *J. Power Sources* **2015,** *293*, 941-945.

63. Rosero-Navarro, N. C.; Kinoshita, T.; Miura, A.; Higuchi, M.; Tadanaga, K., Effect of the binder content on the electrochemical performance of composite cathode using Li_6PS_5Cl precursor solution in an all-solid-state lithium battery. *Ionics* **2017,** *23* (6), 1619-1624.
64. Yubuchi, S.; Uematsu, M.; Deguchi, M.; Hayashi, A.; Tatsumisago, M., Lithium-Ion-Conducting Argyrodite-Type Li_6PS_5X (X = Cl, Br, I) Solid Electrolytes Prepared by a Liquid-Phase Technique Using Ethanol as a Solvent. *ACS Applied Energy Materials* **2018,** *1* (8), 3622-3629.
65. Rosero-Navarro, N. C.; Miura, A.; Tadanaga, K., Composite cathode prepared by argyrodite precursor solution assisted by dispersant agents for bulk-type all-solid-state batteries. *J. Power Sources* **2018,** *396*, 33-40.
66. Chida, S.; Miura, A.; Rosero-Navarro, N. C.; Higuchi, M.; Phuc, N. H. H.; Muto, H.; Matsuda, A.; Tadanaga, K., Liquid-phase synthesis of Li_6PS_5Br using ultrasonication and application to cathode composite electrodes in all-solid-state batteries. *Ceram. Int.* **2018,** *44* (1), 742-746.
67. Yubuchi, S.; Uematsu, M.; Hotehama, C.; Sakuda, A.; Hayashi, A.; Tatsumisago, M., An argyrodite sulfide-based superionic conductor synthesized by a liquid-phase technique with tetrahydrofuran and ethanol. *J. Mater. Chem. A* **2019,** *Accepted*.
68. Phuc, N. H. H.; Morikawa, K.; Mitsuhiro, T.; Muto, H.; Matsuda, A., Synthesis of plate-like Li_3PS_4 solid electrolyte via liquid-phase shaking for all-solid-state lithium batteries. *Ionics* **2017,** *23* (8), 2061-2067.
69. Oh, D. Y.; Kim, D. H.; Jung, S. H.; Han, J.-G.; Choi, N.-S.; Jung, Y. S., Single-step wet-chemical fabrication of sheet-type electrodes from solid-electrolyte precursors for all-solid-state lithium-ion batteries. *J. Mater. Chem. A* **2017,** *5* (39), 20771-20779.
70. Zhang, Q.; Mwizerwa, J. P.; Wan, H. L.; Cai, L. T.; Xu, X. X.; Yao, X. Y., Fe_3S_4@$Li_7P_3S_{11}$ nanocomposites as cathode materials for all-solid-state lithium batteries with improved energy density and low cost. *J. Mater. Chem. A* **2017,** *5* (45), 23919-23925.
71. Xu, R. C.; Wang, X. L.; Zhang, S. Z.; Xia, Y.; Xia, X. H.; Wu, J. B.; Tu, J. P., Rational coating of $Li_7P_3S_{11}$ solid electrolyte on MoS_2 electrode for all-solid-state lithium ion batteries. *J. Power Sources* **2018,** *374*, 107-112.
72. Rosero-Navarro, C.; Miura, A.; Tadanaga, K., Preparation of lithium ion conductive Li_6PS_5Cl solid electrolyte from solution for the fabrication of composite cathode of all-solid-state lithium battery. *J. Sol-Gel Sci. Technol.* **2018,** *Accepted*.
73. Kim, D. H.; Oh, D. Y.; Park, K. H.; Choi, Y. E.; Nam, Y. J.; Lee, H. A.; Lee, S.-M.; Jung, Y. S., Infiltration of Solution-Processable Solid Electrolytes into Conventional Li-Ion-Battery Electrodes for All-Solid-State Li-Ion Batteries. *Nano Lett.* **2017,** *17* (5), 3013-3020.
74. Yubuchi, S.; Hayashi, A.; Tatsumisago, M., Sodium-ion Conducting Na_3PS_4 Electrolyte Synthesized via a Liquid-phase Process Using N-Methylformamide. *Chem. Lett.* **2015,** *44* (7), 884-886.
75. Banerjee, A.; Park, K. H.; Heo, J. W.; Nam, Y. J.; Moon, C. K.; Oh, S. M.; Hong, S. T.; Jung, Y. S., Na_3SbS_4 : A Solution Processable Sodium Superionic Conductor for All-Solid-State Sodium-Ion Batteries. *Angew. Chem.* **2016,** *55* (33), 9634-8.
76. Uematsu, M.; Yubuchi, S.; Noi, K.; Sakuda, A.; Hayashi, A.; Tatsumisago, M., Preparation of Na_3PS_4 electrolyte by liquid-phase process using ether. *Solid State Ionics* **2018,** *320*, 33-37.
77. Kim, T. W.; Park, K. H.; Choi, Y. E.; Lee, J. Y.; Jung, Y. S., Aqueous-solution synthesis of Na_3SbS_4 solid electrolytes for all-solid-state Na-ion batteries. *J. Mater. Chem. A* **2018,** *6* (3), 840-844.
78. Xu, X.; Ai, Q.; Pan, L.; Ma, X.; Zhai, W.; An, Y.; Hou, G.; Chen, J.; Zhang, L.; Si, P.; Lou, J.; Feng, J.; Ci, L., $Li_7P_3S_{11}$ solid electrolyte coating silicon for high-performance lithium-ion batteries. *Electrochim. Acta* **2018,** *276*, 325-332.
79. Momma, K.; Izumi, F., VESTA: a three-dimensional visualization system for electronic and structural analysis. *J. Appl. Crystallogr.* **2008,** *41* (3), 653-658.
80. Yamane, H.; Shibata, M.; Shimane, Y.; Junke, T.; Seino, Y.; Adams, S.; Minami, K.; Hayashi, A.; Tatsumisago, M., Crystal structure of a superionic conductor, $Li_7P_3S_{11}$. *Solid State Ionics* **2007,** *178* (15), 1163-1167.
81. Yao, X.; Liu, D.; Wang, C.; Long, P.; Peng, G.; Hu, Y. S.; Li, H.; Chen, L.; Xu, X., High-Energy All-Solid-State Lithium Batteries with Ultralong Cycle Life. *Nano Lett.* **2016,** *16* (11), 7148-7154.

Highlighted references

[44] This paper describes the suspension synthesis of β-Li_3PS_4 and proposes the the formation of Li_3PS_4·3THF complex as part of the reaction mechanism

[47] This paper describes the suspension synthesis of $Li_7P_3S_{11}$.

[57] This is the first report of liquid-phase reaction as well as dissolution–precipitation for sulfide electrolyte.

[62] This paper describes the dissolution–precipitation of Li_6PS_5Cl through Li_6PS_5Cl–ethanol solution and its application for all-solid-state lithium battery.

[65] The morphology of precipitated Li_6PS_5Cl particles is controlled by dispersant in homogeneous solution.

[68] This paper describes the suspension process for the composite positive electrode of all-solid-state lithium battery.

[73] This paper describes Sheet-type all-solid-state battery fabricated by dissolution–precipitation process.